

Colby



Colby College
Digital Commons @ Colby

Honors Theses


Student Research

2012

The Radon Transform and the Mathematics of Medical Imaging

Jen Beatty
Colby College

Follow this and additional works at: <https://digitalcommons.colby.edu/honorstheses>

 Part of the [Analytical, Diagnostic and Therapeutic Techniques and Equipment Commons](#), and the [Applied Mathematics Commons](#)

Colby College theses are protected by copyright. They may be viewed or downloaded from this site for the purposes of research and scholarship. Reproduction or distribution for commercial purposes is prohibited without written permission of the author.

Recommended Citation

Beatty, Jen, "The Radon Transform and the Mathematics of Medical Imaging" (2012). *Honors Theses*. Paper 646.

<https://digitalcommons.colby.edu/honorstheses/646>

This Honors Thesis (Open Access) is brought to you for free and open access by the Student Research at Digital Commons @ Colby. It has been accepted for inclusion in Honors Theses by an authorized administrator of Digital Commons @ Colby.

**THE RADON TRANSFORM AND THE MATHEMATICS OF MEDICAL
IMAGING**

JEN BEATTY

TABLE OF CONTENTS

1. Introduction	3
2. A Mathematical Model for X-Ray Tomography	6
3. Geometry of Medical Imaging	8
4. The Radon Transform	10
5. The Fourier Transform	12
6. The Central Slice Theorem	13
7. The Backprojection	15
8. Convolution and Low Pass Filters	18
9. Discrete Version	21
10. Conclusion	25
11. Acknowledgements	26
References	26

ABSTRACT. Tomography is the mathematical process of imaging an object via a set of finite slices. In medical imaging, these slices are defined by multiple parallel X-ray beams shot through the object at varying angles. The initial and final intensity of each beam is recorded, and the original image is recreated using this data for multiple slices. I will discuss the central role of the Radon transform and its inversion formula in this recovery process.

1. INTRODUCTION

Tomography is a means of imaging a two- or three- dimensional object from many one-dimensional “slices” of the object. In a CT (computerized tomography) scan, these slices are defined by multiple parallel X-ray beams that are perpendicular to the object. This idea is shown in Figure 1, where a slice is defined by the dark band surrounding the patient’s head. A CT scanner makes two measurements: the initial intensity of each X-ray beam, I_0 , at the radiation source, and the final intensity of each beam, I_1 , at the radiation detector. The changes in intensity for a single beam are dependent on the internal density of the object along the line the X-ray passes through (we shall go into more detail about exactly how this process works later in this section). By changing the orientation of the source and detector we are able to gain more information about the internal density of a single slice by looking at the corresponding intensity changes. The motivating question for this discussion is: how do we use the information measured by a CT scanner (the changes in density) to accurately create a picture of the varying densities along a single slice of our object? If we are able to recreate a single slice, we can then use multiple slices to get an idea about the internal structure of our entire object. As a starting point for our discussion, we will consider a single X-ray beam.

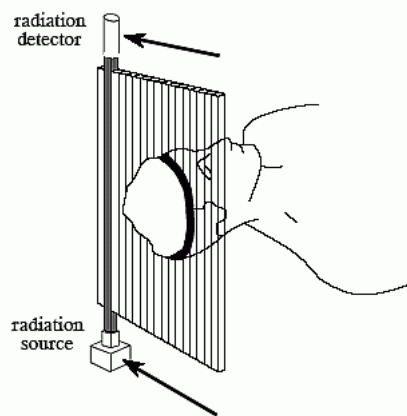


FIGURE 1. CT Example

X-rays are a type of electromagnetic radiation, a form of energy that is dependent on charged particles traveling through space. X-rays have wavelengths between 0.01 to 0.1 nm ($1\text{nm} = 10^{-9}\text{m}$) and corresponding frequencies in the range of 3×10^{16} Hz - 3×10^{19} Hz. We will not focus on the physical properties of X-rays all that much, most important to our discussion is actually the changes in the intensity of a single beam as it comes in contact with a solid object. When an X-ray is shot through an object it loses some of its energy to the surrounding medium. This loss corresponds to a decrease in the *intensity* of the beam.

Intensity is energy flux averaged over the period of the wave and is dependent on both the speed of the wave and the energy density (energy/ unit volume) of the wave. By measuring the initial and final intensities of a single beam, we gain some knowledge about the density of the medium through which it passed. Intuitively it makes sense that a denser object (such as bone) would cause a greater change in the intensity of the beam than would a less dense object (such as human tissue) .

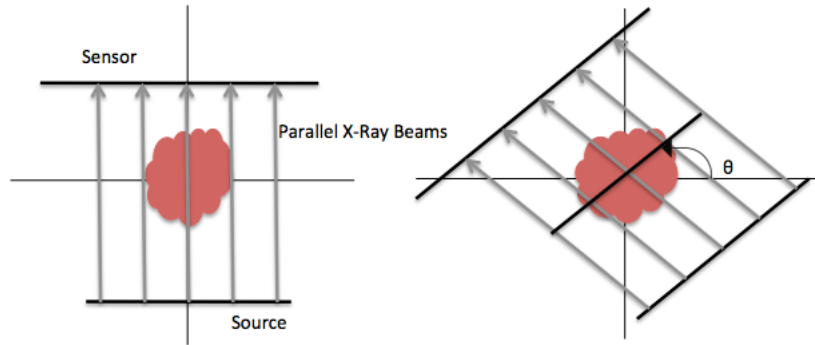


FIGURE 2. Parallel X-Ray Beam Geometry

What about more complex objects, however? In a CT scan a single X-ray beam cross through many different materials such as blood, bone, tissue, etc. This causes the density of the object to vary over the length of the beam and measuring the initial and final intensities of a single beam in one direction does not give us any information about the changing densities along the path of the beam, only the overall loss in intensity. The idea behind tomography is that by measuring the changes in intensity of X-ray beams in many different directions we might be able to compile enough information to determine the different densities of our initial medium. To make these varying measurements, we shall assume a *parallel beam geometry*. This idea is demonstrated in Figure 2, where we have multiple parallel beams creating two different slices; first the beams are perpendicular to the x -axis, then they are rotated through by an angle θ . By changing the angle θ the beams travel along, we are able to create a new slice. There are other beam geometries

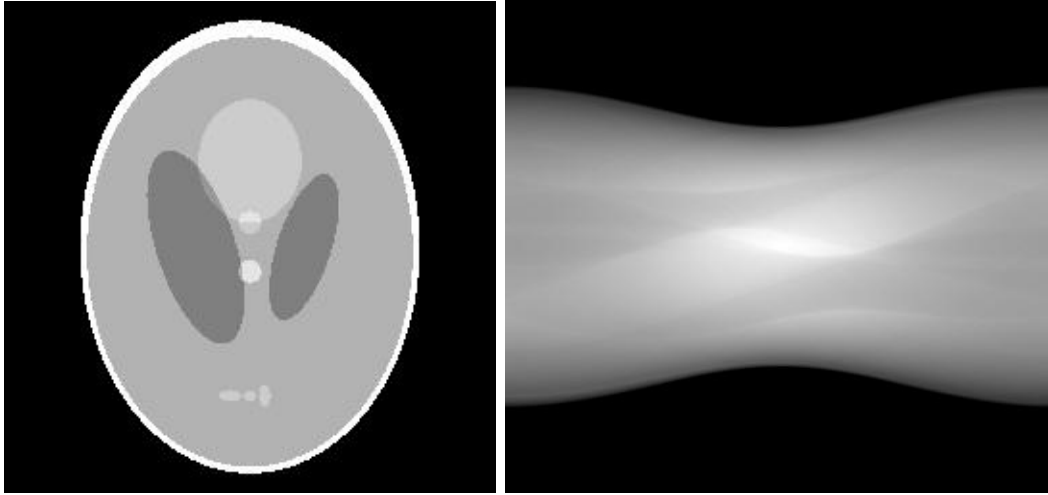


FIGURE 3. Shepp Logan Phantom and Sinogram

used in modern CT scanners such as a fan beam or cone geometry, however we shall limit this discussion to parallel X-ray beams.

The corresponding losses in intensity are given a grayscale value between 0 (black) and 1 (white). A value of 0 corresponds to zero change in intensity and a value of 1 corresponds to the beam being completely absorbed by the medium. The compilation of these varying values creates what is known as a sinogram (Figure 3). A sinogram is a graphical representation of the intensity losses measured by the CT scanner where the vertical axis represents the distance various beams are from the origin and the horizontal axis represents the angle at which the slice is measured. Therefore, a single point in the sinogram represents our measured change in intensity for a given distance and angle. From the information given in a sinogram we are able to recreate the structure of the original object. In Figure 3 we see an example of a sinogram created from a “phantom” image. A phantom image is an object created from predetermined data (i.e., it is a “fake” image). Phantom images are generally used in the testing process for various reconstruction algorithms to determine that any errors in the outcome are due to errors in the algorithm itself and not errors in the data gathering process. The Shepp Logan phantom shown in Figure 3 is the most common phantom used in medical imaging reconstruction.

In order to reconstruct our starting image, however, we need some method of deriving detailed information about the internal density of the medium from the initial and final densities of our various x-ray beams. It is nearly impossible to determine the starting densities of the object merely by inspecting the information shown in the sinogram. Finding a meaningful and useful solution to this problem will be the point of this paper. In order to solve this, however, we will need to make several simplifying (but not highly unreasonable) assumptions about X-ray beams.

- (i) All X-ray beams are *monochromatic* (each photon in the wave propagates at the same frequency and with the same energy level E).
- (ii) All X-ray beams have zero width.
- (iii) X-ray beams are not subject to *refraction* (they do not scatter when they come into contact with a surface) or *diffraction* (they do not bend when they come into contact with a surface).

While these assumptions are not entirely accurate, they are close enough to reality so that, for our purposes, we can take them as fact. Actual CT scanners use corrective algorithms to deal with the refraction and diffraction of some particles in the beam.

The amount of energy lost by an X-ray beam as it travels through a medium is specific to that medium and in particular depends on the density of the medium. We wish to be able to somehow classify the density of the medium in terms of the amount of energy it causes an X-ray beam to lose. This characteristic of a medium is known as its *attenuation coefficient*.

As hinted at earlier in our discussion of the changes in intensity through bone versus tissue, denser objects have a higher attenuation coefficient than less dense objects. In objects of uniform density, the attenuation coefficient is constant for all points $P = (x, y)$. Most interesting objects, however, are not of a uniform density and therefore have a varying attenuation coefficient over a range of P values. Therefore, what we really desire is a means of determining an equation for $A(P)$ which accounts for the varying densities of our medium.

This thesis describes one solution to the inverse problem of solving for the attenuation coefficient in medical imaging. In Section 2 we offer a mathematical model for X-ray tomography and in Sections 3 and 4 we discuss the Radon transform and a parametrization method which presents us with a link between our measured data and the attenuation coefficient we wish to solve for. In Section 5 we introduce the Fourier transform which is a necessary part of the inversion process because of the key role it plays in the Central Slice Theorem discussed in Section 6. Sections 7 and 8 discuss an inversion process known as the backprojection formula and a means of increasing the accuracy of inversion, while Section 9 addresses the discretization of the formulas used previously to make them applicable to real world data.

2. A MATHEMATICAL MODEL FOR X-RAY TOMOGRAPHY

Now that we have an idea of the physical model for CT scans, we shall take a closer look at the mathematical model we will use to determine the attenuation coefficient of our object. In order to do that, however, we will need more mathematical rigorous definitions for the intensity and attenuation coefficient of an object.

Definition 2.1. For a given energy level E of an X-ray beam and a rate of photon propagation $N(x)$, the **intensity** of the beam, $I(x)$, at a distance x from the origin is defined as

$$I(x) = N(x) \cdot E. \quad (2.1)$$

Definition 2.2. The proportion of photons absorbed per millimeter of substance at a distance x from the origin is known as the **attenuation coefficient**, $A(x)$, of the medium.

We know the initial and final intensities, I_0 and I_1 , of a single beam. What we want is to be able to use these intensities to determine the attenuation coefficient over the path of the beam. Fortunately, we can find a relationship between these two values in the Beer-Lambert Law.

Definition 2.3. The **Beer-Lambert Law** states that for a monochromatic, non-refractive, zero-width X-ray beam that transverses a homogenous material along a distance x from the origin, the intensity $I(x)$ is given by

$$I(x) = e^{-A(x)x}. \quad (2.2)$$

As it stands, this equation is not all that useful to us. It gives the attenuation coefficient at a certain point in relation to the intensity at that point, but we only know the value of the intensity at points *outside* our object. What we really want is to be able to find some relationship between the attenuation coefficient inside our object and the change in intensity of the beam. To do this, we shall manipulate equation (2.1) slightly.

Differentiating (2.1) we see:

$$\frac{dI}{dx} = -A(x)I(x).$$

Let $I(x_0) = I_0$ be the initial intensity at x_0 and $I(x_1) = I_1$ be the final intensity at x_1 . We therefore are able to see that

$$\int_{x_0}^{x_1} \frac{dI}{I(x)} = - \int_{x_0}^{x_1} A(x)dx,$$

which, after integration, yields

$$\ln \left(\frac{I_1}{I_0} \right) = - \int_{x_0}^{x_1} A(x)dx.$$

When multiplied by -1 this gives us a very nice final equation relating the initial and final intensities with the attenuation coefficient

$$\ln\left(\frac{I_0}{I_1}\right) = \int_{x_0}^{x_1} A(x)dx. \quad (2.3)$$

Therefore, what CT scan algorithms actually solve for is not the density function of the material but rather its attenuation coefficient. Logically this is not altogether surprising because it seems reasonable that there is a strong relationship between the density of an object and the proportion of photons it attenuates. From now on we shall not concern ourselves with the difference between the density function and the attenuation coefficient of a material and shall discuss them interchangeably.

3. GEOMETRY OF MEDICAL IMAGING

Before going into further analysis of solving equation (2.2) it will be useful for us to spend some time describing the coordinate system that we will be using. The problem with a Cartesian coordinate system is that it is unable to handle vertical lines with an infinite slope (and we certainly do not want to exclude all vertical lines from our CT scan), and a polar coordinate system does not easily lend itself to systems dependent on parallel lines. Therefore we adopt a “point normal” parameterization for a line. We are all familiar with the idea that a line l in \mathbb{R}^2 can be represented by the equation $ax + by = c$ where $a, b, c \in \mathbb{R}$ and $a^2 + b^2 \neq 0$. One could say that a, b , and c parameterize l . Knowing $\sqrt{a^2 + b^2} \neq 0$, we can rewrite the standard equation of a line in the following format

$$\frac{a}{\sqrt{a^2 + b^2}}x + \frac{b}{\sqrt{a^2 + b^2}}y = \frac{c}{\sqrt{a^2 + b^2}}.$$

We now define $\omega = (\omega_1, \omega_2) = \left(\frac{a}{\sqrt{a^2 + b^2}}, \frac{b}{\sqrt{a^2 + b^2}}\right)$ which we can see is a point lying on the unit circle S^1 , for

$$\left(\frac{a}{\sqrt{a^2 + b^2}}\right)^2 + \left(\frac{b}{\sqrt{a^2 + b^2}}\right)^2 = 1.$$

This furthermore implies that $\omega = (\cos \theta, \sin \theta)$ for some $\theta \in [0, 2\pi)$. Letting $t = \left(\frac{c}{\sqrt{a^2 + b^2}}\right)$, we see that we can rewrite l using the inner product $\langle z, \omega \rangle$ where $z = (x, y) \in \mathbb{R}^2$. In other words, we have shown that:

$$\begin{aligned} \langle z, \omega \rangle &= x\omega_1 + y\omega_2 \\ &= \frac{a}{\sqrt{a^2 + b^2}}x + \frac{b}{\sqrt{a^2 + b^2}}y = \frac{c}{\sqrt{a^2 + b^2}} \\ &= x \cos \theta + y \sin \theta = t \end{aligned}$$

Note that in the above equations t and θ are fixed and determine a specific line l in the plane. We therefore can say that t and θ parameterize a line $l_{t,\theta}$ and that z determines specific points on the line l . In other words:

$$l_{t,\theta} = \{z \in \mathbb{R}^2 : \langle z, (\cos \theta, \sin \theta) \rangle = t\}. \quad (3.1)$$

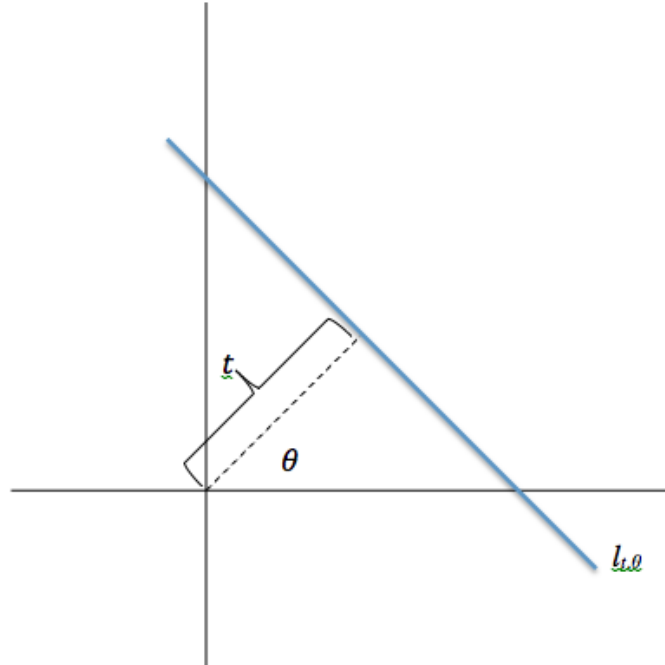


FIGURE 4. Parameterized line $l_{t,\theta}$

Figure 4 offers a visual of what we have done to parameterize the space of all lines. We can imagine that the combination of θ and t define a point $(t \cos \theta, t \sin \theta)$ in space and that as z varies we travel up and down our desired line $l_{t,\theta}$. The line $l_{t,\theta}$ is the line that is perpendicular to the vector $\langle t \cos \theta, t \sin \theta \rangle$ through the point $(t \cos \theta, t \sin \theta)$.

We now offer an alternative definition for a specific point on the line $l_{t,\theta}$ (although this may seem a bit redundant now, this additional notation will become useful in future derivations). To do this, we note that $\langle -\sin \theta, \cos \theta \rangle$ is perpendicular to $\langle \cos \theta, \sin \theta \rangle$. Therefore we can describe a particular point (x, y) on $l_{t,\theta}$ in terms of a real number s as follows:

$$(x(s), y(s)) = \langle t \cos \theta, t \sin \theta \rangle + \langle -s \sin \theta, s \cos \theta \rangle, \text{ for } s \in \mathbb{R}.$$

In the above equation, each t and θ determine a particular line l . This leads to an alternative definition for the set of points that make up a line $l_{t,\theta}$:

$$l_{t,\theta} = (x(s), y(s)) = \{(t \cos \theta - s \sin \theta, t \sin \theta + s \cos \theta) : s \in \mathbb{R}\}. \quad (3.2)$$

4. THE RADON TRANSFORM

We are ready to introduce some mathematical tools that will be central to solving for the attenuation coefficient in equation (2.3).

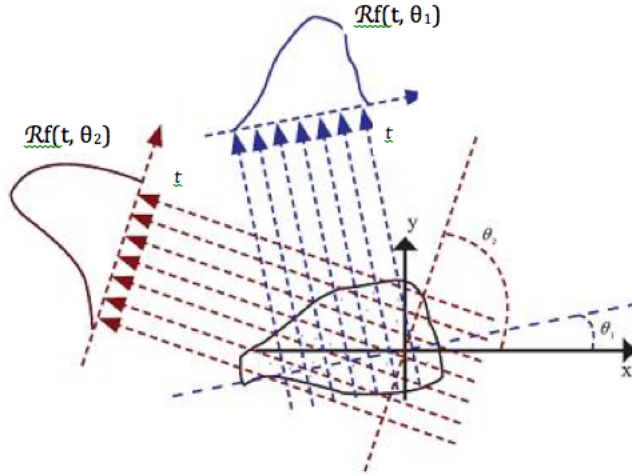
Definition 4.1. For a function $f(t, \theta)$ defined on \mathbb{R}^2 with compact support the **Radon transform** of f , denoted by $\mathcal{R}f$, is defined for $t \in \mathbb{R}$ and $\theta \in (0, 2\pi]$ as

$$\mathcal{R}f(t, \theta) = \int_{-\infty}^{\infty} f(x(s), y(s)) ds. \quad (4.1)$$

A function with *compact support* is one that takes the value zero everywhere outside of a compact set. This is a reasonable requirement for a medical imaging problem because we are only dealing with finite areas (or slices) of some object. Recall that our goal is to determine the attenuation coefficient of our object which is related to the object's density. Therefore, since we are only dealing with finite slices, there will be some finite region outside of which the attenuation coefficient must equal zero.

The Radon transform offers a means of determining the total density of a certain function f along a given line l . This line l is determined by an angle θ from the x -axis and a distance t from the origin as described in equation (3.1). As shown in Figure 5 if we take the Radon transform along multiple lines at varying angles (here θ_1 and θ_2), we are able to determine multiple density functions for our object. Intuitively we can interpret the Radon transform as a “smeared” version of our initial object. Suppose the blob like region represented in Figure 5 were an ink blot; if we were to smear this blot along varying lines in the direction θ_1 , we can expect that the wider regions of the ink blot would correspond to a larger region than smaller regions, which is exactly what we see.

The integral $\mathcal{R}f(t, \theta)$ represents the right half of equation (2.3). Recall that in this equation $A(x)$ is unknown and $\ln(\frac{I_0}{I_1})$ is measured information. In other words, $\ln(\frac{I_0}{I_1})$ is the Radon transform, and therefore the Radon transform represents known, measured data.

FIGURE 5. Radon Transform for θ_1 and θ_2

The goal now is to find some type of inversion formula for the Radon transform that will allow us to recover our starting function f (or, in the context of medical imaging, $A(x)$). To do this, it will be useful to note several properties of the Radon transform.

Properties 4.2. For real constants α , β , and continuous functions f and g on \mathbb{R}^2 with compact support:

- (i) $\mathcal{R}(\alpha f + \beta g) = \alpha \mathcal{R}f + \beta \mathcal{R}g$
- (ii) $\mathcal{R}f(t, \theta) = \mathcal{R}f(-t, -\theta)$
- (iii) $\mathcal{R}f(t, \theta) = \int_{-\infty}^{\infty} f(x(s), y(s)) ds = \int_{-\infty}^{\infty} f(t \cos \theta - s \sin \theta, t \sin \theta + s \cos \theta) ds$

Property (i) tells us that the Radon transform is linear, (ii) that it is even, and (iii) utilizes the equivalent geometric expressions used in the previous section to create different expressions for the same transform which we will use interchangeably depending on which best suits our needs.

We furthermore define the *natural domain* of the Radon transform as the set of functions f on \mathbb{R}^2 such that

$$\int_{-\infty}^{\infty} |f(x(s), y(s))| ds < \infty.$$

That is, we restrict our domain to the set of *absolutely integrable functions*.

We have now devised a new way of stating our initial problem of solving for the attenuation coefficient function $A(x)$ in a mathematical framework. The Radon transform is the mathematical name for equation (2.3). Therefore to recover $A(x)$, we need to find an inversion formula for the Radon transform. Unfortunately, there is no single straightforward answer to this solution. To get an actual inversion formula we will have to delve into some more advanced mathematics.

5. THE FOURIER TRANSFORM

Definition 5.1. For a given absolutely integrable function f on \mathbf{R} the **Fourier Transform** of f , denoted by $\mathcal{F}f$ is defined for every real number ξ as

$$\mathcal{F}f(\xi) = \int_{-\infty}^{\infty} f(x)e^{-2\pi i x \xi} dx. \quad (5.1)$$

Although it might not seem relevant at the present, we will make extensive use of the Fourier transform and its inverse formula in our search for a solution to our medical imaging problem. The Fourier transform is used frequently in signal analysis and offers a means of changing a function of time into a function of frequency, the variable x represents time in seconds and the variable ξ represents the frequency of the function in Hertz. There exists an alternate definition that uses the angular frequency, ω , where $\omega = 2\pi\xi$, giving us

$$\mathcal{F}f(\omega) = \int_{-\infty}^{\infty} f(x)e^{-i\omega x} dx. \quad (5.2)$$

We will primarily deal with this second definition of the Fourier transform throughout our discussion as it is the form more commonly used in engineering and medical imaging.

We now note that compactly supported functions are a subset of a larger space of functions, the Schwartz Space ($\mathcal{S}(\mathbb{R}^n)$), which consists of all infinitely differentiable functions on \mathbb{R}^n such that for all $k, l \geq 0$:

$$\sup_{x \in \mathbb{R}^n} \left| x^k \frac{\partial^l}{\partial x^l} f(x) \right| < \infty$$

These functions are also known as *rapidly decreasing functions*. Henceforth we shall assume that \mathcal{S} denotes the two dimensional Schwartz space ($\mathcal{S}(\mathbb{R}^2)$) since that is the dimension we are interested in for our attenuation problem.

We limit our discussion to functions within \mathcal{S} because there are several nice properties about this domain. The first is that within this domain there exists a bijective relationship between the Fourier transform and its inverse; the second is that the Fourier transform of a Schwartz function is still a Schwartz function; and the third is that we are allowed to change the order of integration for multiple integrals if $f \in \mathcal{S}$.

As we did with the Radon transform, we shall list several properties of the Fourier transform.

Properties 5.2. For real constants α and β and absolutely integrable functions f and g :

$$(i) \quad \mathcal{F}(\alpha f + \beta g) = \alpha \mathcal{F}(f) + \beta \mathcal{F}(g)$$

$$(ii) \quad \mathcal{F}f(\omega) < \infty$$

As was hinted at earlier, we will also make use of the inverse Fourier transform.

Definition 5.3. For an absolutely integrable function f we define the **inverse Fourier transform** of f , denoted by $\mathcal{F}^{-1}f$, evaluated at x as

$$\mathcal{F}^{-1}f(x) = \frac{1}{2\pi} \int_{-\infty}^{\infty} f(\omega) e^{i\omega x} d\omega.$$

This immediately leads us to the following theorem.

Theorem 5.4. For a function $f \in \mathcal{S}$ the **Fourier Inversion Theorem** states that, for all x :

$$\mathcal{F}^{-1}(\mathcal{F}f)(x) = f(x).$$

So far, we have only addressed the Fourier transform in one dimension. There exist corresponding definitions in higher dimensions, although for our purposes we will only utilize the two dimensional analogs.

Definition 5.5. For an absolutely integrable function g defined on \mathbb{R}^2 , the **2 dimensional Fourier transform** of g , denoted by \mathcal{F}_2g , is defined for all $(X, Y) \in \mathbb{R}^2$ as

$$\mathcal{F}_2g(X, Y) = \int_{-\infty}^{\infty} \int_{-\infty}^{\infty} g(x, y) e^{-i(xX+yY)} dx dy. \quad (5.3)$$

We similarly define the inverse Fourier transform on \mathbb{R}^2 .

Definition 5.6. For an absolutely integrable function g defined on \mathbb{R}^2 the **2 dimensional inverse Fourier transform** at a point (x, y) , denoted by $\mathcal{F}_2^{-1}g(x, y)$ is given as

$$\mathcal{F}_2^{-1}g(x, y) = \frac{1}{4\pi^2} \int_{-\infty}^{\infty} \int_{-\infty}^{\infty} g(X, Y) e^{i(xX+yY)} dx dy. \quad (5.4)$$

6. THE CENTRAL SLICE THEOREM

There is just one more big theorem we need to discuss before we can begin the actual process of inverting the Radon transform and recovering our attenuation coefficient. The *central slice theorem* gives us a remarkable relationship between the two dimensional Fourier transform and the one dimensional Fourier transform of the Radon transform.

Theorem 6.1. For an absolutely integrable function f defined on \mathbb{R}^2 and all $S \in \mathbb{R}$ and $\theta \in [0, 2\pi)$,

$$\mathcal{F}_2 f(S \cos \theta, S \sin \theta) = \mathcal{F}(\mathcal{R}f)(S, \theta).$$

Proof. We first recall that the two dimensional Fourier transform of $f(x, y)$ is given by:

$$\mathcal{F}_2 f(x, y) = \int_{-\infty}^{\infty} \int_{-\infty}^{\infty} f(x, y) e^{-iS(x \cos \theta + y \sin \theta)} dx dy \quad (6.1)$$

We now implement a change of variables here according to the coordinate system we defined in section 3. Recall that when we parameterized the line $l_{t, \theta}$ we discovered that we could say the following for $s \in \mathbb{R}$:

$$x(s) = t \cos \theta - s \sin \theta, \quad y(s) = t \sin \theta + s \cos \theta, \quad t = x \cos \theta + y \sin \theta$$

Looking at the determinant of the Jacobian for $x(s)$ and $y(s)$:

$$\det \begin{bmatrix} \frac{\partial x}{\partial t} & \frac{\partial x}{\partial s} \\ \frac{\partial y}{\partial t} & \frac{\partial y}{\partial s} \end{bmatrix} = 1$$

we see that we can say that $ds dt = dx dy$. We therefore rewrite the right half of equation (6.1) in terms of the variables s, t

$$\int_{-\infty}^{\infty} \int_{-\infty}^{\infty} f(t \cos \theta - s \sin \theta, t \sin \theta + s \cos \theta) e^{-iSt} ds dt.$$

Because e^{iSt} has no dependence on s , we are able to rearrange the above integral as follows:

$$\int_{-\infty}^{\infty} \left(\int_{-\infty}^{\infty} f(t \cos \theta - s \sin \theta, t \sin \theta + s \cos \theta) ds \right) e^{-iSt} dt.$$

This inner integral is exactly the Radon transform of $f(t, \theta)$, implying that

$$\int_{-\infty}^{\infty} (\mathcal{R}f(t, \theta)) e^{-iSt} dt.$$

Which in turn is the Fourier transform of $\mathcal{R}f(S, \theta)$, and we conclude our proof. \square

The central slice theorem (also known as the Fourier slice theorem or the slice projection theorem) is a link between the one and two dimensional Fourier transforms. The theorem tells us that the one dimensional Fourier transform of a projected function (the Radon transform) is equal to the two dimensional Fourier transform of the original function taken on the slice through the origin parallel to the line we projected our function on. This idea is demonstrated in Figure 3. In the left part of the figure we start with a function $F(x, y)$ and apply the Radon transform to get a projection g to which we then apply the Fourier transform, receiving the orange G function at the top of the figure. In the right half we take the 2 dimensional Fourier transform of the orange slice of $F(x, y)$ parallel to the projection line. This 2 dimensional Fourier transform also equals the orange G function depicted at the top of the image.

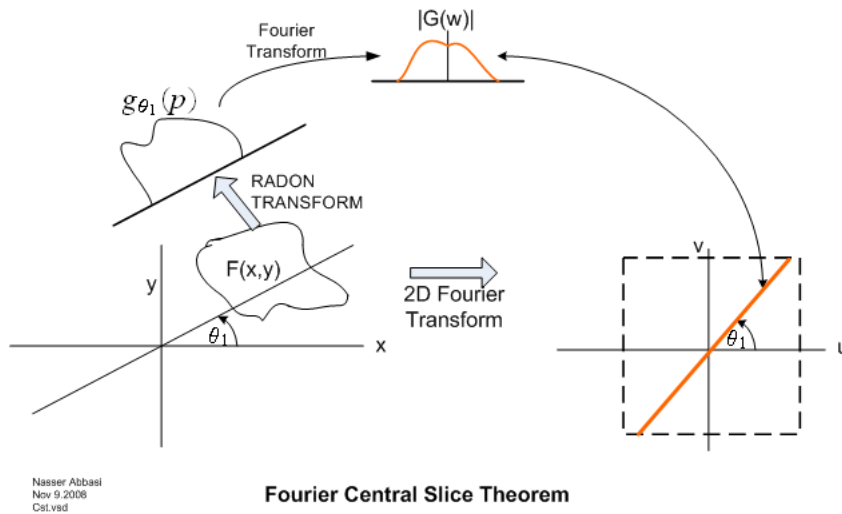


FIGURE 6. Central Slice Theorem

This theory can also be extended to higher dimensions, but for our purposes in solving the inverse problem of finding the attenuation coefficient the two dimensional interpretation will suffice.

7. THE BACKPROJECTION

We are now finally ready to make a first attempt at recovering our attenuation coefficient function. Recall that, physically speaking, the Radon transform $\mathcal{R}f(t, \theta)$ gives us the total density of the object f along a line $l_{t, \theta}$. We have determined this density by measuring the initial and final intensities of an X-ray beam shot through the object along this line. By doing this along multiple different lines, we are able to create a single slice of our starting object and by varying the angle θ of these X-rays we are able to define many slices.

If we are somehow able to "backproject" these densities onto the plane, perhaps we will be able to recreate our starting object. Intuitively we can think of this process as taking the sinogram data and "unsmearing" it back onto the plane.

Definition 7.1. Let $h = h(t, \theta)$. We define the **backprojection**, $\mathcal{B}h$, at a point (x, y) as

$$\mathcal{B}h(x, y) = \frac{1}{\pi} \int_0^\pi h(x \cos \theta + y \sin \theta, \theta) d\theta.$$

Applying this backprojection formula to the Radon transform, we receive the following:

$$\mathcal{B}\mathcal{R}f(x, y) = \frac{1}{\pi} \int_0^\pi \mathcal{R}f(x \cos \theta + y \sin \theta, \theta) d\theta. \quad (7.1)$$

In the context of medical imaging, f represents our attenuation coefficient function.

We are able to backproject over the slices we have measured. As demonstrated in Figure 7, backprojecting in only a few directions θ is an incredibly inaccurate way of recreating even a simple object. However, even if we significantly increase the number of backprojections we use (say to 1000 directions), there is still a large amount of noise blurring our recreated image. As it turns out, no matter how many directions we try to backproject in, we will still not be able to perfectly recreate our image using the backprojection formula of equation (7.1). For this process to be at all useful, we will need to derive a way to filter out some of the noise the backprojection formula seems to create in our picture and get a smoother representation of our object.

To this end, we define a *filtered backprojection formula*.

Theorem 7.2. For an absolutely integrable function f defined on \mathbb{R}^2

$$f(x, y) = \frac{1}{2} \mathcal{B} \{ \mathcal{F}^{-1} [|S| \mathcal{F}(\mathcal{R}f)(S, \theta)] \} (x, y). \quad (7.2)$$

Proof. We first note the fact that, for the 2 dimensional Fourier transform and its inverse:

$$\begin{aligned} f(x, y) &= \mathcal{F}_2^{-1} \mathcal{F}_2 f(x, y) \\ &= \frac{1}{4\pi^2} \int_{-\infty}^{\infty} \int_{-\infty}^{\infty} \mathcal{F}_2 f(X, Y) e^{i(xX+yY)} dX dY. \end{aligned} \quad (7.3)$$

We now will use a change of variables from Cartesian (X, Y) to polar coordinates (S, θ) where $X = S \cos \theta$ and $Y = S \sin \theta$ with $S \in \mathbb{R}$ and $\theta \in [0, \pi]$. This gives the following Jacobian determinant:

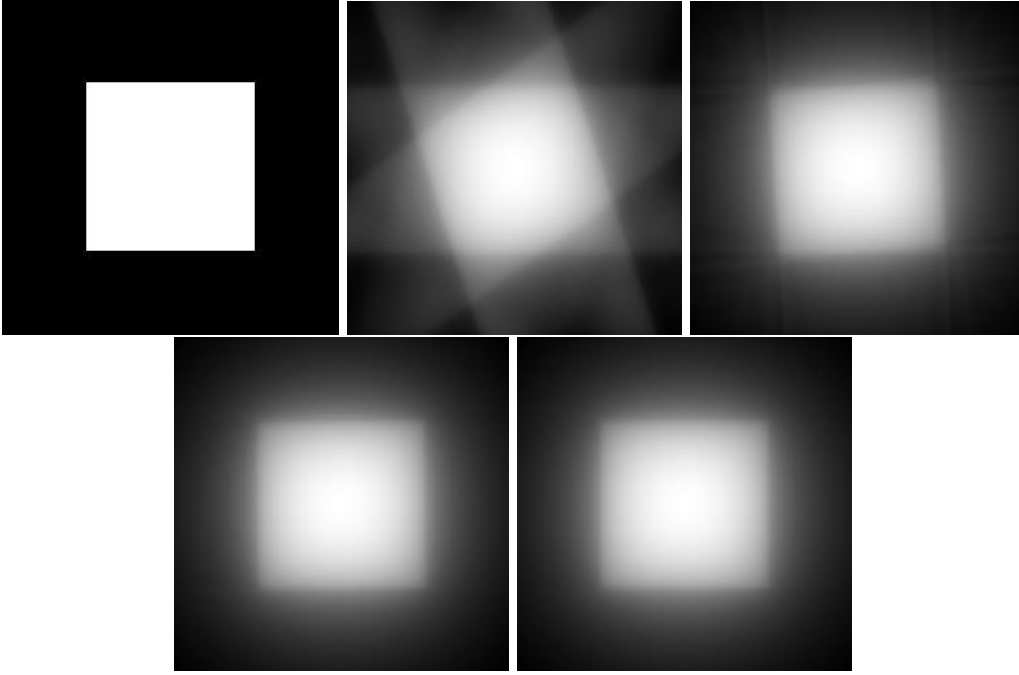


FIGURE 7. Backprojection of a Square in 5, 25, 100, and 1000 Directions

$$\det \begin{bmatrix} \frac{\partial X}{\partial S} & \frac{\partial X}{\partial \theta} \\ \frac{\partial Y}{\partial S} & \frac{\partial Y}{\partial \theta} \end{bmatrix} = |S|$$

Which tells us that $dXdY = |S|dSd\theta$. Incorporating this new change of variables equation (7.2) becomes:

$$\frac{1}{4\pi^2} \int_0^\pi \int_{-\infty}^\infty \mathcal{F}_2 f(S \cos \theta, S \sin \theta) e^{iS(x \cos \theta + y \sin \theta)} |S| dS d\theta.$$

And using the central slice theorem we see that the above equation is in fact equal to

$$\frac{1}{4\pi^2} \int_0^\pi \int_{-\infty}^\infty \mathcal{F}(\mathcal{R}f(S, \theta)) e^{iS(x \cos \theta + y \sin \theta)} |S| dS d\theta. \quad (7.4)$$

Now let us take a closer look at the inner integral of equation (7.4) and note the following:

$$\begin{aligned}
& \int_{-\infty}^{\infty} \mathcal{F}(\mathcal{R}f(S, \theta)) e^{iS(x \cos \theta + y \sin \theta)} |S| dS \\
&= 2\pi \left(\frac{1}{2\pi} \int_{-\infty}^{\infty} \mathcal{F}(\mathcal{R}f(S, \theta)) e^{iS(x \cos \theta + y \sin \theta)} |S| dS \right) \\
&= 2\pi \mathcal{F}^{-1} [|S| \mathcal{F}(\mathcal{R}f)(S, \theta)] (x \cos \theta + y \sin \theta, \theta)
\end{aligned}$$

That is, the inner integral of equation (7.4) is 2π times the inverse of the Fourier transform of $|S| \mathcal{F}(\mathcal{R}f)(S, \theta)$ at the point $(x \cos \theta + y \sin \theta, \theta)$. We are then able to see that (7.4) in fact equals

$$\frac{1}{2\pi} \int_0^\pi \mathcal{F}^{-1} [|S| \mathcal{F}(\mathcal{R}f)(S, \theta)] (x \cos \theta + y \sin \theta, \theta) d\theta.$$

Finally we see that the above integral is $\frac{1}{2}$ the backprojection given in definition (7.1) for $\mathcal{F}^{-1} [|S| \mathcal{F}(\mathcal{R}f)(S, \theta)]$. We therefore simplify the above equation to

$$\frac{1}{2} \mathcal{B} \{ \mathcal{F}^{-1} [|S| \mathcal{F}(\mathcal{R}f)(S, \theta)] \} (x, y).$$

Which leads us to our desired conclusion that

$$f(x, y) = \frac{1}{2} \mathcal{B} \{ \mathcal{F}^{-1} [|S| \mathcal{F}(\mathcal{R}f)(S, \theta)] \} (x, y).$$

□

The important factor in this formula is the $|S|$ multiplier that occurs between the Fourier transform and its inverse. Without this factor these two terms would cancel each other out and we would be left with the standard backprojection formula for the Radon transform we encountered earlier which, as we saw, does not directly give us back $f(x, y)$. We call this additional $|S|$ a filter to the Radon transform, giving us the name for the filtered backprojection formula.

8. CONVOLUTION AND LOW PASS FILTERS

Here we shall examine the role of the filtering factor $|S|$ in the filtered backprojection formula given in equation (7.2). In order to do that, however, we must first introduce the notion of the *convolution* of two functions.

Definition 8.1. For two integrable functions f, g defined on \mathbb{R} we define the **convolution** of f and g , denoted by $f \star g$, as

$$(f \star g)(x) = \int_{-\infty}^{\infty} f(t)g(x-t)dt$$

where $x \in \mathcal{R}$.

We can easily extend this definition to 2 dimensional space. For polar functions, we only take the integral over the radial variable while for Cartesian functions we integrate over both variables. Explicit definitions are given as follows:

Definition 8.2. For integrable polar functions $f(t, \theta)$ and $g(t, \theta)$ we define the **convolution** of f and g as

$$(f \star g)(t, \theta) = \int_{-\infty}^{\infty} f(s, \theta) \cdot g(t-s, \theta)ds$$

For integrable functions F, G on \mathbb{R}^2 , we define the **convolution** of F and G as

$$(F \star G)(x, y) = \int_{-\infty}^{\infty} \int_{-\infty}^{\infty} F(s, t) \cdot G(x-s, y-t)dsdt.$$

Convolution is a mathematical method of averaging one function, f , with the shifting of another function, g . In the convolution $f \star g$, the function g is translated across the function f and the resulting function is dependent on the area of overlap during this translation. In a sense we can view g as a filter we are using to average f over a certain interval. The filtering function acts as a smoother for the noisy data given by the original function.

Properties 8.3. For integrable functions f, g, h on \mathbb{R} and constants $\alpha, \beta \in \mathbb{R}$:

- (i) $f \star g = g \star f$
- (ii) $f \star (\alpha g + \beta h) = \alpha(f \star g) + \beta(f \star h)$
- (iii) $\mathcal{F}f \cdot \mathcal{F}g = \mathcal{F}(f \star g)$
- (iv) $(\mathcal{B}g \star f)(X, Y) = \mathcal{B}(g \star \mathcal{R}f)(X, Y)$.

We now reconsider the filtered backprojection formula from theorem (7.2):

$$f(x, y) = \frac{1}{2} \mathcal{B} \{ \mathcal{F}^{-1} [|S| \mathcal{F}(\mathcal{R}f)(S, \theta)] \} (x, y).$$

This is, admittedly, a rather ugly equation to deal with. Fully expanded it would include several infinite integrals, which is problematic since we are only dealing with a finite set of data. It would be nice if we could somehow further simplify this to a more useful form. To that end, we shall make a seemingly odd assumption. Suppose that there was some function, call it $\phi(t)$, whose Fourier transform equaled our filtering factor $|S|$. That is, suppose we had a function $\phi(t)$ such that $\mathcal{F}\phi(S) = |S|$. More simply put, suppose we knew of a function whose Fourier transform equaled the absolute value function. Then we would be able to rewrite the backprojection as

$$f(x, y) = \frac{1}{2} \mathcal{B} \{ \mathcal{F}^{-1} [\mathcal{F} \phi \cdot \mathcal{F}(\mathcal{R}f)(S, \theta)] \} (x, y). \quad (8.1)$$

However the right half of equation (8.1) contains a product of Fourier transforms, which we know to be equal to the convolution of the functions being transformed as shown in property (iii). We therefore have

$$f(x, y) = \frac{1}{2} \mathcal{B} \{ \mathcal{F}^{-1} [\mathcal{F}(\phi \star \mathcal{R}f)(S, \theta)] \} (x, y).$$

But this is merely the inverse Fourier transform of the Fourier transform, which we know returns our starting function. This leads us to the much simpler filtered backprojection formula

$$f(x, y) = \frac{1}{2} \mathcal{B}(\phi \star \mathcal{R}f)(x, y). \quad (8.2)$$

Equation (8.2) looks much nicer than our original filtered backprojection formula and doesn't seem that difficult to apply. Physically speaking, $\mathcal{R}f$ is our measured data and (8.2) only requires us to filter it with our new function ϕ and then apply the backprojection formula which is a relatively straightforward integral.

Unfortunately, there is no such function ϕ whose Fourier transform is exactly equal to the absolute value. Consider the function $\mathcal{F}\phi$:

$$\mathcal{F}\phi(\omega) = \int_{-\infty}^{\infty} \phi(x) e^{-i\omega x} dx$$

We can see that, as $\omega \rightarrow \infty$, $\mathcal{F}\phi(\omega) \rightarrow 0$ (note the negative exponential). However, for the absolute value function, $|\omega|$, as $\omega \rightarrow \infty$, $|\omega| \rightarrow \infty$. Therefore we, are unable to find a function ϕ such that for all ω , $\mathcal{F}\phi(\omega) = |\omega|$.

All our previous work was not in waste, however. Let us consider what type of functions we have restricted our interest to. We are only looking at our function on a finite interval and are in fact assuming it to be zero outside of that interval. If we extend this idea to the Fourier transform, we find that we want to focus our attention on *band limited functions*.

Definition 8.4. *A function ϕ is said to be a **band limited function** if, for some real number $L > 0$:*

$$\mathcal{F}\phi(\omega) = \int_{-\infty}^{\infty} \phi(x) e^{-i\omega x} dx = 0 \text{ for all } \omega \notin [-L, L] \quad (8.3)$$

The filtering factor $|S|$ serves to magnify the $\mathcal{F}(\mathcal{R}f)$ term in the original filtered backprojection formula (7.2). In practice $\mathcal{F}(\mathcal{R}f)$ is very sensitive to high frequencies. By focusing

our attention on the lower frequencies via a band limited function ϕ , we are able to avoid this issue. Our goal will be to replace S with what is known as a *low pass filter* (denoted by S') which takes into account the affects of lower frequencies but attenuates higher frequencies. This function S' needs to have compact support and be of the form $S' = \mathcal{F}\phi$ (on a compact interval).

The cost of using this $S'(\omega)$ is that we no longer have the equality shown in equation (8.2). Rather, we receive the following:

$$f(x, y) \approx \frac{1}{2}\mathcal{B}(\mathcal{F}^{-1}S' \star \mathcal{R}f)(x, y). \tag{8.4}$$

Generally speaking, most low pass filters are of the form $S'(\omega) = |\omega| \cdot F(\omega) \cdot \square_L(\omega)$ where $L > 0$ defines the region we are filtering over. Different functions for F determine the precise characteristics of the filer, and $\square_L(\omega)$ is defined as follows:

$$\square_L(\omega) = \begin{cases} 1 & \text{if } |\omega| \leq L \\ 0 & \text{if } |\omega| > L \end{cases}$$

We shall introduce two common filters used in digital imaging and signal processing, the *Ram-Lak filter* and *Hann filter*.

The *Ram-Lak filter*:

$$S'(\omega) = |\omega| \cdot \square_L(\omega) = \begin{cases} |\omega| & \text{if } |\omega| \leq L \\ 0 & \text{if } |\omega| > L \end{cases}$$

The Ram-Lak filter is the basis for many of the other filters used in signal analysis for it simply replaces the $F(\omega)$ function with the constant 1 function. Other filters, such as the Hann filter, generally consist of multiples of sin or cos to filter out unwanted noise.

The *Hann filter*:

$$S'(\omega) = |\omega| \cdot \frac{1}{2} \left(1 + \cos \frac{2\pi\omega}{L} \right) \cdot \square_L(\omega)$$

The Hann filter uses the Hann function $(1 + \cos \frac{2\pi\omega}{L})$ as its $F(\omega)$ and its effectiveness is demonstrated in the sinogram and backprojection of Johann Radon shown in Figure 5.

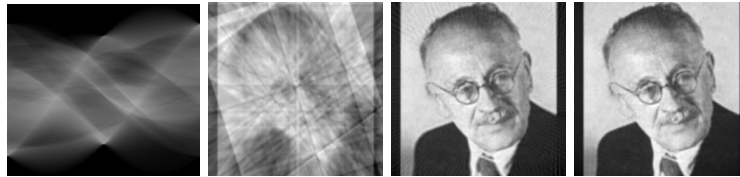


FIGURE 8. Sinogram and Hann Filter Backprojection for 10, 100, and 1000 Backprojections

9. DISCRETE VERSION

Thus far we have been dealing almost exclusively with continuous integrals for the Radon transform, Fourier transform, and backprojection formulas. In practice, however, we only have a finite set of data to work with. Therefore we will need to form discrete versions of all the formulas we have used in our filtered backprojection.

A discrete function is one that is only defined on a countable set. For our purposes, we shall be looking at discrete functions defined on finite sets (the set being composed of the lines we took our intensity measurements on). Let g_n denote the discrete function g at the value n . Because we know this discrete function at a finite set of points, say N , we can say that $g = g_n : 0 \leq n \leq N - 1$. If we wish to extend this definition to all integers, we can simply “repeat” our function over and over again; that is, we can make it periodic with period N . This extension will be useful for some of the discrete formulas we will encounter.

Suppose we are taking measurements at P different angles θ and that for each angle have $2 \cdot M + 1$ beams spaced a distance d apart. Then we can define particular values θ_k and t_j as

$$\theta_k = \left\{ \frac{k\pi}{P} : 0 \leq k \leq P - 1 \right\},$$

$$t_j = \{j \cdot d : -M \leq j \leq M\}.$$

Which allows us to define particular line as l_{t_j, θ_k} . We therefore define the discrete Radon transform as follows:

Definition 9.1. For an absolutely integrable function f and $0 \leq k \leq P$ and $-M \leq j \leq M$, ($P, M > 0$), we define the **discrete Radon transform** of f , denoted $\mathcal{R}_D f$, as

$$\mathcal{R}_D f_{j,k} = \mathcal{R}f(t_j, \theta_k). \quad (9.1)$$

To implement the filtered backprojection formula (8.4), we shall also need to define the convolution of two discrete functions.

Definition 9.2. For two N -periodic discrete functions f and g , we define the **discrete convolution** of f and g , denoted $f \bar{*} g$, as

$$(f \bar{*} g)_m = \sum_{j=0}^{N-1} f_j \cdot g_{(m-j)}, \text{ for } m \in \mathbb{Z} \quad (9.2)$$

Clearly, we shall also need the discrete Fourier transform.

Definition 9.3. Given an N -periodic discrete function f we define the **discrete Fourier transform** of f , denoted $\mathcal{F}_D f$, as

$$(\mathcal{F}_D f)_j = \sum_{k=0}^{N-1} f_k e^{i2\pi k j / N} \text{ for } j = 0, 1, \dots, (N-1). \quad (9.3)$$

It is worth noting that the N -periodicity of f allows us to replace the bounds in the summation by any set of integers of length $(N-1)$. Given the above definition, it should not come as a surprise that we define the discrete inverse Fourier transform as follows:

Definition 9.4. Given an N -periodic discrete function g the **discrete inverse Fourier transform** of g , denoted $\mathcal{F}_D^{-1} g$, is defined as

$$(\mathcal{F}_D^{-1} g)_n = \frac{1}{N} \sum_{k=0}^{N-1} g_k e^{i2\pi k n / N}, \text{ for } n = 0, 1, \dots, (N-1). \quad (9.4)$$

We note that several of the same properties of the Fourier transform we defined in the continuous setting also apply to the discrete case with slight modifications:

Properties 9.5. For N -periodic discrete functions f and g :

- (i) $\mathcal{F}_D(f \bar{\star} g) = (\mathcal{F}_D f) \cdot (\mathcal{F}_D g)$
- (ii) $\mathcal{F}_D(f \cdot g) = \frac{1}{N} (\mathcal{F}_D f) \bar{\star} (\mathcal{F}_D g)$
- (iii) $\mathcal{F}_D^{-1}(\mathcal{F}_D f)_n = f_n$ for all $n \in \mathbb{Z}$

We are now ready to attack the discretization of the backprojection formula itself. Recall that the backprojection formula was defined as an integral from 0 to π over $d\theta$. In the discrete case we have replaced this continuous $d\theta$ with $k\pi/P$ for $0 \leq k \leq (P-1)$. This leads to the following definition for the discrete backprojection:

Definition 9.6. Given a discrete function h we define the **discrete backprojection** of h , denoted $\mathcal{B}_D h$, as

$$\mathcal{B}_D h(x, y) = \left(\frac{1}{N} \right) \sum_{k=0}^{N-1} h\left(x \cos \frac{k\pi}{N} + y \sin \frac{k\pi}{N}, k\pi/N\right). \quad (9.5)$$

Recall our final form for the filtered backprojection formula in equation (8.4)

$$f(x, y) \approx \frac{1}{2} \mathcal{B}(\mathcal{F}^{-1} S' \star \mathcal{R} f)(x, y).$$

To form the discrete version of this equation, we see that we need to apply the following formula:

$$f(x, y) \approx \frac{1}{2} \mathcal{B}_D(\mathcal{F}_D^{-1} S' \bar{\star} \mathcal{R}_D f)(x, y).$$

And now, we run into a slight problem. $\mathcal{R}_D f$ is measured data based on the initial and final intensities of a single X-ray beam. We defined the locations of different beams (and therefore different slices) using a coordinate system perpendicular to polar coordinates based on discrete angles θ and distances t . Looking at equation (9.5), however, we see that we will need to sum over h at various points (x, y) in the Cartesian coordinate system to create a rectangular grayscale grid that represents our original object. The polar and Cartesian coordinate systems do not necessarily match up as nicely as we wish them to, and therefore we must *interpolate* the missing data points. Interpolation is the process of making a continuous (or at a minimum piecewise continuous) function out of a discrete set of values. There are many different ways to interpolate a function (cubic spline, Lagrange, etc.), each with its own set of gains and drawbacks. For our purposes we shall define a general type of interpolation based on a weighting function W which determines how we shall choose our interpolated points. We will not define a particular weighting function, W , since the details of how the values are interpolated is not as important to us as is the knowledge that we are able to fill in the “gaps” in our data.

Definition 9.7. *For a given weighting function W and an N -periodic discrete function g , the **W -interpolation** of g is defined as*

$$\mathcal{I}_W(g)(x) = \sum_n g(n) \cdot W\left(\frac{x}{d} - n\right), \text{ for } -\infty < x < \infty. \quad (9.6)$$

Now that we have covered all the various parts of equation (8.2) in a discrete setting and dealt with the interpolation issue, we are able to give a discrete reconstruction algorithm to solve for the attenuation coefficient using a discrete set of data.

Here we are interpolating the function $(\mathcal{F}_D^{-1} S') \bar{\star} (\mathcal{R}_D f)(jd, k\pi/N)$ (that is, are filling in the gaps after filtering the Radon transform). Let us define this interpolated function as \mathcal{I} . This leads to the following reconstruction formula:

$$\begin{aligned} f(x_m, y_n) &\approx \frac{1}{2} \mathcal{B}_D((\mathcal{F}_D^{-1} S') \bar{\star} (\mathcal{R}_D f))(jd, k\pi/N) \\ &\approx \frac{1}{2} \mathcal{B}_D \mathcal{I}(x_m, y_n) \\ &= \frac{1}{2N} \sum_{k=0}^{N-1} \mathcal{I}\left(x_m \cos \frac{k\pi}{N} + y_n \sin \frac{k\pi}{N}, \frac{k\pi}{N}\right). \end{aligned} \quad (9.7)$$

Equation (9.7) accounts for the discrete nature of our real world data and addresses the issues (such as not enough data) that arise from only having a finite number of measurements.

We therefore offer the following completed algorithm for solving the inverse problem of CT scan medical imaging using the Radon transform.

- (1) Given a set $2 \cdot M + 1$ X-ray beams each spaced a distance d apart, measure the initial and final intensities, (I_0, I_1) , of each beam.
- (2) Repeat this process for P different angles θ .
- (3) Choose a filter function $\mathcal{F}_D^{-1} S'$.
- (4) Choose a weighting function for interpolation, $\mathcal{I}_W(g)(x)$
- (5) Apply the reconstruction formula described in equation (9.7)

10. CONCLUSION

We have shown the mathematical background for the images created by CT scans and explained the central role of the Radon (and consequently Fourier) transform in this process. While the algorithm described here is not the only method for reconstructing a three-dimensional image from projected two-dimensional slices, it did serve as a starting point for research into the field of medical imaging. In particular, there are reconstruction methods based on a specific function which mimics the backprojection formula [4] or there are recent numerical algorithms which are much more efficient in reconstruction [1], although, as in our method derived here, every option has its own strengths and weaknesses.

11. ACKNOWLEDGEMENTS

I would like to thank my thesis advisor, Alan Von Herrmann, for his guidance during my thesis research and my second reader, Fernando Gouvêa, for his invaluable help during my research.

REFERENCES

- [1] Bal, G., Moireau, P. "Fast numerical inversion of the attenuated Radon transform with full and partial measurements," *Inverse Problems*, Institute of Physics Publishing, 20(2004), pp1137-1164.
- [2] Freeman, T.G., "The Mathematics of Medical Imaging", Springer Undergraduate Texts in Mathematics and Technology, 2010.
- [3] Smith, S., "The Scientist and Engineer's Guide to Signal Processing," California Technical Publishing, 1997.
- [4] Nievergelt, Y. "Elementary Inversion of Radon's Transform," *SIAM Review*, 28(1986), pp 79-84.
- [5] Tianhu, L. "Statistics of Medical Imaging," Taylor and Franics Group, 2012.